CHEMICAL ENGINEERING TRANSACTIONS
VOL. 103, 2023
A publication of AIDIC
The Italian Association of Chemical Engineering
Online at www.cetjournal.it
Guest Editors: Petar S. Varbanov, Panos Seferlis, Yee Van Fan, Athanasios Papadopoulos

ISBN 979-12-81206-02-1; **ISSN** 2283-9216
DOI: 10.3303/CET23103071

Thermohydraulic Effects of Scaling in Flat Plate Solar Collector Networks

Hebert Lugo-Granados[a,*], Lázaro Canizalez-Dávalos[a], Martín Picón-Núñez[b]

[a]Autonomous University of Zacatecas, Department of Chemical Engineering, Zacatecas, México
[b]Department of Chemical Engineering, University of Guanajuato, Noria Alta s/n, Guanajuato, Gto., Mexico
lugh871024@gmail.com

This work presents a theoretical study of fouling in flat plate solar collectors. The thermal performance of solar collectors is determined by operating variables such as surface area, network configuration, and flow distribution, as well as external factors such as solar radiation and weather conditions. However, in most flat plate solar collectors, where water is the working fluid, it is common for scaling to occur, reducing heat transfer and increasing pressure drop. Fouling in pipes increases resistance to heat transfer and increases pressure drop. Consequently, the thermal performance of solar collectors decreases while increasing pumping power. An inadequate design of a network of solar collectors causes poor fluid distribution, which affects thermal performance. In channels with low water flow rates, the fluid reaches higher temperatures, which increases the rate of scaling deposition on the surfaces of the pipes. There are few studies on fouling in solar collectors and its effect on thermal and hydraulic performance. Therefore, the use of a model to predict fouling and the development of a mathematical model to determine the flow distribution in the network will allow for the identification of improved network structure designs. It is shown that in retrofit, reduction of free flow area by 40 %, reduces fouling deposition and pressure drop due to scaling but only reduces the maximum outlet temperature by 0.55 °C between the clean and fouled conditions.

1. Introduction

Fouling is a common operating problem that appears in any heat transfer process. Most fouling mechanisms are related to operational parameters such as fluid velocity and temperature. In fouling due to scaling, salt precipitation takes place due to the presence of inverse solubility salts such as calcium carbonate, where water is the heat transfer medium. Scaling, as any other fouling mechanism, causes the gradual deterioration of the thermal and hydraulic performance of the heat transfer device. Solar water heaters of the flat plate type are devices prone to scaling deposition.

The literature on this subject is not abundant, which indicates the need for further research to increase the experimental data on fouling and its thermal and hydraulic effects. Arunachala et al. (2012) studied the effect of scaling in natural convection solar collectors. Later, Arunachala et al. (2015) presented and experimental and theoretical study of fouling on a forced convection system, where they determined, on the thermal aspect, the variation of the heat loss coefficient, the variation of the instantaneous thermal efficiency, and on the hydraulic aspect, the variations of the water mass flow rate resulting from the increased pressure drop due to the growth of a layer of scale within the tubes. Harrison (2012) examined the maximum stagnation temperature of flat plate solar collectors finding that at high temperatures, fouling and corrosion can rise significantly. Researchers have also studied the use of antifoulant in flat plate collectors. For instance, Ren et al. (2020) used a ternary nickel-tungsten-phosphorus (Ni-W-P) coating to inhibit $CaCO_3$ deposition.

The limited number of fouling studies on solar collector systems focus on the experimental quantification of the depositions and their thermal effects; however, no studies have been published on the combined thermo-hydraulic effects and their implications on the design and how these findings can be implemented in the retrofit of existing large solar collector fields. This work seeks to fill this gap by studying the thermohydraulic performance of such systems.

Paper Received: 13 April 2023; Revised: 27 June 2023; Accepted: 30 June 2023
Please cite this article as: Lugo-Granados H., Canizalez-Dávalos L., Picón-Núñez M., 2023, Thermohydraulic Effects of Scaling in Flat Plate Solar Collector Networks, Chemical Engineering Transactions, 103, 421-426 DOI:10.3303/CET23103071

2. Methodology

In this work, the model used to predict fouling deposition due to scaling in flat plate collectors is the one presented by Lugo-Granados and Picón-Núñez (2018). The model was validated against experimental scaling data reported in other works. The model predicts calcium carbonate deposition on the inner surface of the tubes using Eq(1).

$$\dot{m}_d = \frac{\beta}{2}\left(\frac{\beta}{\alpha\, k_r} + (C_1 + C_2) - \sqrt{\frac{[\beta + (C_{1+}C_2)\,\alpha\, k_r]^2 + 4\,\alpha^2\, {k_r}^2\left(K_{sp} - [C_1][C_2]\right)}{\alpha^2\, {k_r}^2}}\right) \tag{1}$$

The model allows for the determination of the mass flux $\dot{m}_d$ (kg/m^2 s) of $CaCO_3$ that gets deposited inside the tubes. It includes all the parameters that take part in scaling formation such as: water quality (pH and calcium carbonate concentration) that affect the solubility K_{sp} (kg^2/m^6) of $CaCO_3$ in water, calcium concentration Ca^{2+} is represented by C_1 (kg/m^3) and carbonate concentration, CO_3^{2-} (C_2) (kg/m^3). The term α represents the dimensionless correction factor due to inertial and viscous forces (Lugo-Granados and Picón-Núñez, 2019). The model also includes design variables such as temperature, that determines the rate of the chemical reaction, k_r (m^2/kg s) for scale formation, and the fluid velocity that affects the rate of scale deposition. The latter is expressed in the form of mass transfer coefficients from the fluid to the surface, β (m/s). As fouling builds up, the inner tube surface roughness and its diameter change causing increase in drop pressure.
From the mass flux deposited with time $\dot{m}_d$ (kg/m^2 s) the fouling resistance can be calculated as given by Eq(2), which depends on the mass removal rate, $\dot{m}_r$ (kg/m^2 s), density of the fouling material ρ_f (kg/m^3) and its thermal conductivity, λ_f (W/m K) for $CaCO_3$.

$$\frac{dR_s}{dt} = \frac{\dot{m}_d - \dot{m}_r}{\rho_f \lambda_f} \tag{2}$$

2.1 Thermal resistance.

The thermal resistance due to fouling directly affects the thermal performance of solar collectors reducing the amount of heat absorbed by the working fluid, Q_u (W) given by Eq(3). The absorbed heat is only a fraction of the net heat absorbed by the plate which is represented by the heat removal factor (Eq(4)) (Duffie and Beckman, 2013).

$$Q_u = \dot{m}_f\, C_p (T_i - T_o) \tag{3}$$

$$Q_u = F_R A_s \left[I_G(\tau\alpha_c) - U_c A_s \left(T_{pm} - T_a\right)\right] \tag{4}$$

Where $\dot{m}_f$ (kg/s) is the mass flow rate of water inside the tubes, C_p (kJ/kg°C) is the heat capacity, T_i and T_0 (°C) are the tube inlet and outlet temperatures, F_R is the heat removal factor from the plate to the fluid, (T_{pm}-T_a) is the temperature difference between the plate and ambient (°C), (α_c and τ) are the absorbance and transmittance of the transparent cover, I_G is the intensity of the solar radiation (W/m^2) and As is the heat transfer area. The heat removal factor F_R, Eq(5), depends on the efficiency factor of the collector F´ (Eq(6)), and this in turn on the thermal effectiveness of the metal fin F_A, Eq(8).

$$F_R = \frac{\dot{m}_f C_P}{A_s\, U_c}\left[1 - e^{\frac{-A_s\, U_c F'}{\dot{m}_f C_P}}\right] \tag{5}$$

The collector efficiency factor depends on the overall heat transfer coefficient U_c (W/m^2°C) and the heat transfer resistances to heat transfer from the plate to the working fluid including the resistance between the plate and the tube C_b (m^2 °C /W) described in Eq(7), due to the tube thickness R_t (m^2 °C/W), the layer of fouling R_s (m^2 °C/W), and the resistance due to convection between the inner tube wall and the fluid R_h (m^2 K/W). In solar collector modeling, the resistance due to fouling is seldom considered.

$$F' = \frac{1/U_c}{S\left[\frac{1}{U_c[d_0 + F_A(S - d_0)]} + \frac{1}{C_b} + \frac{R_h}{\pi d} + \frac{R_t}{\pi d} + \frac{R_s}{\pi d}\right]} \tag{6}$$

$$C_b = \frac{k_b W}{\gamma} \tag{7}$$

Where k_b is the thermal conductivity, W (m) is the width, and γ (m) is the thickness of the joint between the plate and the tube. d and d_0 (m) are the inner and out tube diameter, S (m) is the distance between tubes. The fin efficiency (FA) is expressed by Eq(8).

$$F_A = \frac{Tanh[M(S-d_0)/2]}{M(S-d_0)/2} \tag{8}$$

While M (m^{-1}) is expressed in Eq(9), where K_s (W/m/°C) and δ (m) are the thermal conductivity and the thickness of the plate.

$$M = \sqrt{\frac{U_c}{K_s \delta}} \tag{9}$$

While the thermal efficiency (η) is expressed by Eq(10).

$$\eta = \frac{Q_u}{I_G A_s} \tag{10}$$

2.2 Hydraulic resistance.

The thermal resistance created by fouling increases the hydraulic resistance. Eq(11) shows that thickness of the fouling deposits x_f (m) is proportional to the thermal resistance. The thickness of the fouling layer causes the reduction of the tube diameter altering the roughness which increase the fluid velocity and pressure drop.

$$x_f = R_s \lambda_f \tag{11}$$

Within a network of solar collectors, the total pressure drop can be calculated from Eq(12), where it is seen that it is proportional to hydraulic resistances K_i (kPa s^2/m^6) and the square of the volumetric flow rate $\dot{V}$ (m^3/s).

$$\Delta P_T = \dot{V}^2 \sum_{i=1}^{n} K_i \tag{12}$$

The main hydraulic resistances are due to friction K_1 (kPa s^2/m^6) along the length of the pipes and the loss generated due to fittings, K_2 (kPa s^2/m^6) such as elbows, valves, and other fittings.

$$K_1 = \frac{8L}{\pi^2 d^5} f \tag{13}$$

$$K_2 = \frac{8\rho}{\pi^2 d^5} k_r \tag{14}$$

From Eq(13) and Eq(14) it is seen that as the diameter reduces, the flow resistance increases, giving rise to increased pressure drop (Eq(12)). The term f is the friction factor along the pipe, k_r is the resistance factor for each of the fittings, L (m) and d (m) are the length and diameter of the tube.
The configuration of a network of solar collectors determines its pressure drop. The configuration can be series, parallel or a combination of both (Lugo-Granados et al. (2021). In a parallel configuration the total flow rate is equal to the sum of the flow through each collector Eq(15), while the pressure drop is the same in each collector (Eq(16)).

$$\dot{V}_T = \sum_{i=1}^{i=n} V_i \tag{15}$$

$$\Delta P_1 = \Delta P_2 = \Delta P_3 \tag{16}$$

When a centrifugal pump feeds a solar collector network, the flow rate is determined by the amount of pressure drop. For a typical centrifugal pump, when the pressure drop increases, the mass flow rate tends to reduce.

3. Results

The design and construction features of an existing thermo-solar plant is considered as a case study (García-Valladares, 2019). The plant is used to provide the heat load for fruit dehydration and contains 40 collectors

divided in 4 rows, each with 10 collectors. Each row is configured in two series of 5 collectors connected in parallel as shown in Figure 1. Where Ts is the outlet temperature network.

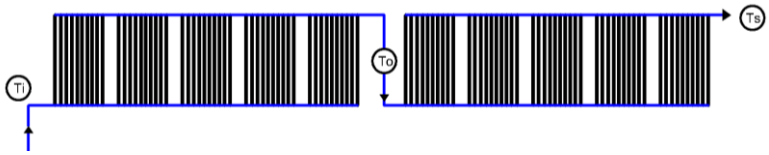

Figure 1: Single row in the collector network structure

Table 1 shows the construction features of the flat plate collectors. The solar time is considered during the month of September from 6:00 h to 18:00 h, when the maximum solar radiation reached at 12:00 h is 1,067 W/m^2.

Table 1: Construction features of the flat plate solar collectors

Dimensions	Length 2,099 [mm]	width 1,196 [mm]	Surface area 2.31 [m^2]
Absorber tube	Number of tubes 11	External diameter 10 [mm]	Internal diameter 8 [mm]
Cover	Material Tempered solar glass	Transmittance 0.91	Thickness 4 [mm]
Surface	Absorptivity 0.95	Emissivity 0.4 [mm]	Thickness 0.05
Headers	Number of headers 2	External diameter 22 [mm]	Internal diameter 20 [mm]
Insulation	Bottom insulation thickness 44 [mm]	Side insulation thickness 25 [mm]	Material Polyurethane+mineral wool

3.1 Thermal model validation

Experimental data from García-Valladares (2019) were used to validate the model. Figure 2(a) shows the experimental data (red points) and the theoretical results (blue line). It is observed that the theoretical results are very close to the experimental ones with a maximum error 10 % as shown in Figure 2(b). These results demonstrate the accuracy of the thermal model.

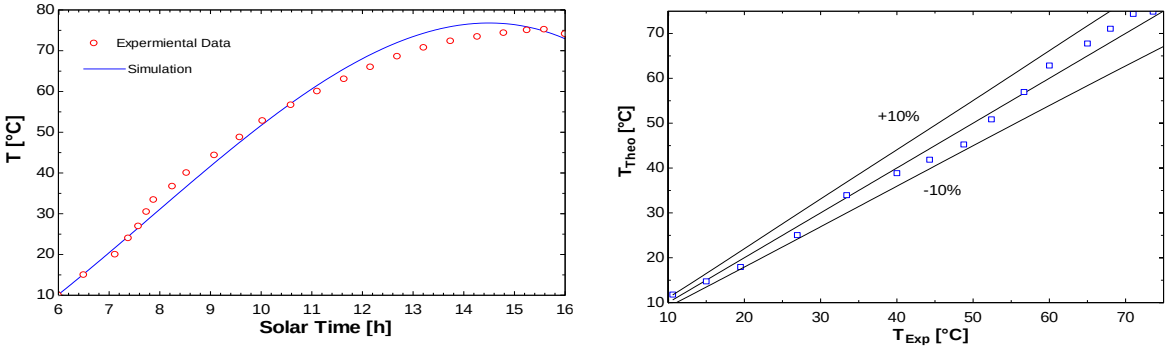

(a) (b)

Figure 2: Theoretical and experimental results: a) outlet network temperature vs. solar time, b) error between predicted and measured outlet temperature

3.2 Fouling and its thermo-hydraulic effects

To simplify the analysis, in this section only the single row of 10 collectors depicted in Figure 1 is analysed. The effect of the thermal resistance due to fouling on the thermal and hydraulic performance is determined. The calculations are made for the following conditions: inlet temperature T_i=55 °C, solar radiation of I_G=900 W/m^2 and volumetric flow rate of $\dot{V}$=3.78 l/min. Calculations show that after a period of operation of six months has reached a value of 1.5x10^{-3} m^{2}K/W (due to space limitations the fouling resistance vs time plot is not included). For the same conditions, Figures 3(a) and 3(b) show the variation of outlet temperature and pressure drop with

respect to time. The temperature drop after six months is 1.5 °C while the pressure drop increases 1.2 kPa. These results indicate that fouling has a larger adverse effect on the hydraulic performance.

Figures 4(a) and 4(b) show the outlet temperature profile and thermal efficiency profile, during the day after six months operation with (blue line) and without (black line) fouling. The highest temperature difference in the day with and without scaling is about 3 °C (Figure 4(a)). In normal operation without fouling, the thermal efficiency drops as the collector temperature increases; but as the presence of fouling keeps these temperatures at lower levels, the drop in efficiency is less pronounced reaching a lower value of 44 % against 36 % for the no fouling condition.

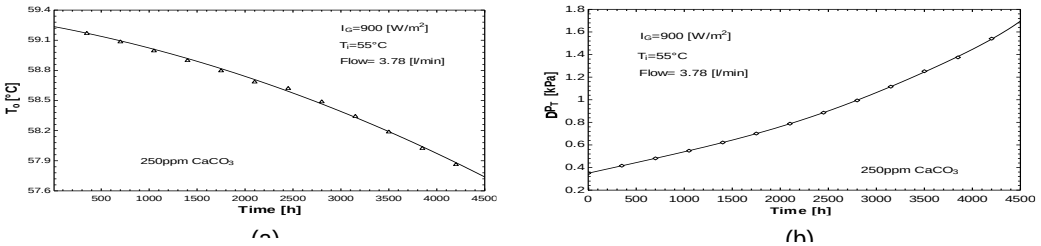

Figure 3: Collector thermal and hydraulic performance: a) deterioration of outlet temperature with time, b) increase of pressure drop with time

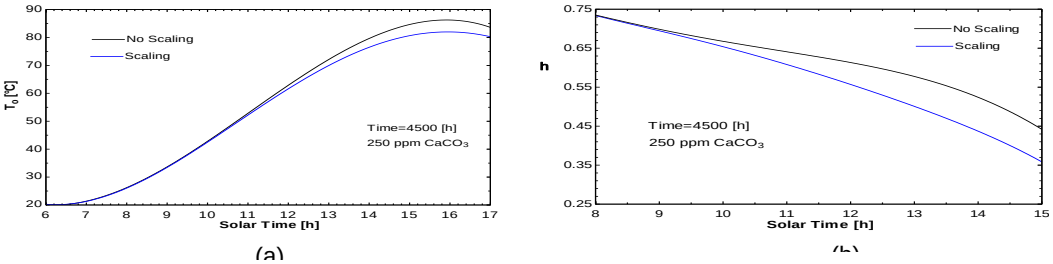

Figure 4: Thermal performance during the day after six months operation: a) outlet temperature, b) thermal efficiency

3.3 Network retrofit

Based on the connection that exists between fouling rate and fluid velocity, a new network structure was analysed to demonstrate the beneficial effect of reducing fouling. The network structure of each section was analysed reducing the number of collectors in parallel from 5 to 3 (reducing the free flow area by 40 %) which resulted in a change on the flow velocity. Figure 5(a) shows the new pressure drop vs. time considering fouling for the two configurations. When the number of collectors in parallel is 3, the pressure drop is initially larger due to the increased flow velocity; however, as time goes on and reaches 5,500 h operation, the pressure drop has not grown as in the case of the 5 collectors in parallel, where the pressure drop has increased due to the higher fouling rates.

Figure 5(b) compares the outlet temperature versus time for the two network structures for an inlet temperature of Ti=65 °C, a volumetric flow rate of 3.5 L/min and a solar radiation of I_G=900 W/m^{2}K. The analysis is done for an 18-month period. With a 5 parallel collector network, the outlet temperature is higher compared to the 3-collector network since in the former, the fluid flows at lower velocity; however, as time goes on, its temperature reduces at a higher rate due to the higher fouling rate. The temperature drop in the 5-collector network is 1.35 °C and in the 3-collector network the drop is 0.55 °C.

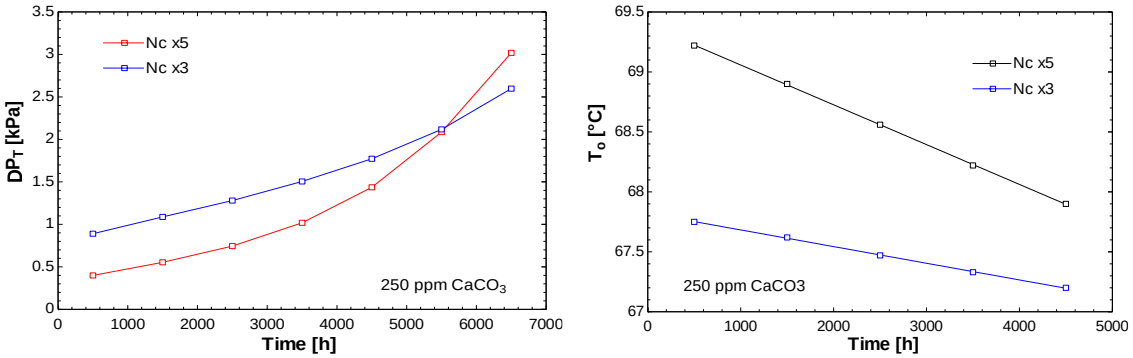

Figure 5: Thermal performance comparison between the two network configurations: a) Pressure drop vs. time, b) outlet temperature vs. time

4. Conclusions

This work uses a fouling model to predict the scaling formation in networks of flat plate solar collectors. The thermohydraulic model incorporates fouling to determine the effect on outlet temperature and pressure drop with time. Prediction of the accumulation of scaling with time allows to find the time for which the thermal performance decay has reached a minimum acceptable value which can be an indication of the need for maintenance. This paper has shown that knowledge of scaling formation can be used in design to reduce the impact of fouling on the thermal and hydraulic performance of the system. The results of this work indicate that the larger adverse effect of fouling is on the hydraulic performance and apart from salt concentration, fluid velocity is one of the most important factors to be considered in design. The main difference between the 5-parallel-collector network compared with a 3-parallel-collector structure is the fluid velocity. With time, the lower velocity system (5 parallel-collector) tends to accelerate the formation of fouling. After six months of operation, the pressure drop is higher due to fouling, increasing 5.25 times the original value with a maximum outlet temperature reduction of 1.3 °C. The 3-parallel-collector structure increases its pressure drop only 2.3 times with a temperature reduction of 0.1 °C after six-month operation. In retrofit, the search for higher fluid velocity must guide the modifications at the expense of higher pressure drop and pumping costs in the first few months; however, after six months the increment in pressure drop is less pronounced.

References

Arunachala U.C., Sreepathi L.K., Bhatt S. M., 2012, Analytical studies on drop of H-W-B constants due to scaling in natural circulation flat plate solar water heater, International Journal of Sustainable Energy, 33, 192-202.

Arunachala U.C., Siddhartha Bhatt M., Sreepathi L.K., 2015, Analytical and experimental investigation to determine the variation of Hottel–Whillier–Bliss constants for a scaled forced circulation flat-plate solar Water heater, Journal of Solar Energy Engineering, 137, 051011.

Duffie J.A., Beckman W.A., 2013, Flat-Plate Collectors, In: Solar Engineering of Thermal Processes, John Wiley & Sons, 4th Ed, Hoboken, New Jersey, United States, 236-319.

García-Valladares O., Pilatowsky-Figueroa I., Ortiz-Rodríguez N., Menchaca-Valdez C., 2019, Solar thermal dehydrating plant for agricultural products installed in Zacatecas, México, WEENTECH Proceedings in Energy, 5, 01-19.

Harrison S.J., Cynthia A., Cruickshank, 2012, Limiting stagnation temperature in flat-plate solar collectors, Energy Procedia, 30, 793-804.

Lugo-Granados H., Picón-Núñez M., 2018, Modelling scaling growth in heat transfer surfaces and its application on the design of heat exchangers, Energy, 160, 845-854.

Lugo-Granados H., Picón-Núñez M., 2019, Incorporating the use of a fouling model in the design and operation of cooling networks. Chemical Engineering Transactions, 76, 43-48.

Lugo-Granados H., Canizalez-Dávalos L., Picón-Núñez M., 2021, Comprehensive analysis of the thermohydraulic performance of cooling networks subject to fouling and undergoing retrofit projects. Energy & Environment, 32, 1414-1436.

Ren L., Cheng Y., Yang J., Wang Q., 2020, Study on heat transfer performance and anti-fouling mechanism of ternary Ni-W-P coating, Applied Sciences, 10, 3905.